Available online at www.sciencedirect.com
SCIENCE DIRECT
Polymer 46 (2005) 2276–2284
polymer
www.elsevier.com/locate/polymer

Optical and thermo-optical properties of space durable polymer/carbon nanotube films: experimental results and empirical equations ☆

Joseph G. Smith Jr[a,*], John W. Connell[a], Kent A. Watson[c], Paul M. Danehy[b]

[a]NASA Langley Research Center, Advanced Materials and Processing Branch, Mail Stop 226, Hampton, VA 23681-2199, USA
[b]NASA Langley Research Center, Advanced Sensing and Optical Measurement Branch, Mail Stop 493, Hampton, VA 23681-2199, USA
[c]National Institute of Aerospace, 144 Research Drive, Hampton, VA 23666, USA

Received 20 August 2004; received in revised form 6 January 2005; accepted 12 January 2005
Available online 2 February 2005

Abstract

The incorporation of purified high-pressure carbon monoxide prepared single-walled carbon nanotubes (HiPco SWNTs) into the bulk of space environmentally durable polymers at loading levels ≥ 0.05 wt% has afforded thin films with surface and volume resistivities sufficient for electrostatic charge mitigation. However, the optical transparency at 500 nm decreased and the solar absorptivity increased with increased SWNT loading. Besides showing a loading dependency, these properties were also dependent upon film thickness. The absorbance of the films at 500 nm as a function of SWNT loading and film thickness was determined to follow the classic Beer–Lambert law. Based on these results, a simple empirical relationship was derived to provide a predictive approximation of these properties. The molar absorptivity determined for the purified HiPco SWNTs dispersed in the polymer by this simple treatment was of the same order of magnitude to reported solution determined values for HiPco SWNTs.

Keywords: Low color polyimides; Carbon nanotubes; Beer–Lambert law

1. Introduction

Space durable polymeric films are one of several enabling technologies for Gossamer spacecraft [1]. These vehicles are large, deployable, and ultra-lightweight and would be partially constructed of polymer films. To be durable to the space environment, the film needs to exhibit resistance to electrons, protons, and ultraviolet (UV) and vacuum UV radiation. Due to their exceptional physical and mechanical properties as well as radiation resistance, aromatic polyimides are excellent materials for space applications. Respectable space environmental durability has been attained by proper choice of the constituent monomers [2,3].

For some space applications, the film must also possess low solar absorptivity and optical transparency across the visible spectrum (particularly at 500 nm), and high thermal emissivity (ε). Optical transparency at 500 nm is of interest since this is the wavelength at which the solar maximum occurs. Solar absorptivity (α) pertains to the fraction of incoming solar energy that is absorbed by the film and is typically low for a low color film. The ε is a measure of the film's ability to radiate energy from the film surface. Films that exhibit low α and high ε are desirable since little radiation would be absorbed while most of the radiation impinging upon it would be radiated away from the surface. It is known that these properties are dependent upon film thickness.

In addition to the aforementioned properties, intrinsic electrical conductivity is needed to mitigate electrostatic charge (ESC) accumulation. ESC build-up occurs due to the exposure of insulating materials (i.e. polymers) to a charged orbital environment. When discharge occurs, damage to surrounding materials and electronics on the spacecraft can result. The level of surface resistivity required to mitigate ESC accumulation is in the range of 10^6–10^{10} Ω/sq [4]. One means of achieving this level of surface resistivity with

* Corresponding author. Tel.: +1 757 864 4297; fax: +1 757 864 8312.
E-mail address: joseph.g.smith@nasa.gov (J.G. Smith).

0032-3861/$ - see front matter Crown Copyright © 2005 Published by Elsevier Ltd. All rights reserved.
doi:10.1016/j.polymer.2005.01.022

potentially little detriment to the optical and thermo-optical properties (α and ε) is by the use of single walled carbon nanotubes (SWNTs). SWNTs are attractive based on the following general reasons: (1) their high aspect ratio, implying that a relatively low loading level would be needed to reach the electrical percolation threshold, (2) due to the low loading levels needed for electrical percolation they would presumably have a negligible effect upon α, ε, and the optical properties of the base polymer, and (3) their high intrinsic electrical conductivity. However, these desirable properties of SWNTs are dependent upon the preparative process, any purification and/or functionalization, chirality, sizes, etc.

SWNTs have been incorporated into the bulk [5–10] of space durable polymers (e.g. TOR-NC, LaRC™ CP-2, and modified LaRC™ CP-2) as well as applied as a surface coating [11] to afford films that possess sufficient intrinsic conductivity for ESC mitigation. Bulk inclusion of SWNTs provided films that exhibited both surface and volume conductivity. Surface coating afforded only one conductive side with the bulk and opposing side being insulative. This surface coating process resulted in a thin layer of Bucky paper being applied to the polymer surface.

It was found that the surface coating of SWNTs on the polymer had a negligible effect upon the optical transparency, α, and ε compared to the pristine material while providing sufficient conductivity [11]. However, bulk inclusion of SWNTs at loading levels necessary to reach the electrical percolation threshold caused significant darkening resulting in increased absorbance (at 500 nm), α, and ε for films of approximately the same thickness [5,7, 10]. An initial plot of the absorbance at 500 nm and α data of these nanocomposites vs. wt% SWNT loading was found to obey the classic Beer's law equation. This adherence to Beer's law has also been observed for SWNTs (produced by the HiPco process) that were 'dissolved' or 'suspended' in 1,2-dichlorobenzene [12] and for functionalized SWNTs (produced by arc discharge) dissolved in solution [13]. Light scattering due to SWNT bundles affected the results as evident by the non-zero y-intercept. Additionally, results for the film samples previously described were affected by reflectivity and scattering losses at the polymer–air interface [10].

Due to the initial adherence of the nanocomposite films in Ref. [10] to Beer's law, it was of interest to further examine these materials and attempt to develop an empirical equation for absorbance (at 500 nm) and α for these particular nanocomposites. The generation of empirical equations for these two macroscopic properties is important given that ultra-thin films (<3 μm in thickness) would be needed for proposed Gossamer structures. Even though these equations would be dependent on this particular polymer and batch of SWNTs, the method employed in developing them could be useful in treating the optical and α data for other low color polymer-SWNT nanocomposites.

In this work, additional nanocomposite films were prepared to evaluate thickness effects upon the optical transparency at 500 nm, α, and ε with respect to the pristine polymer and the nanocomposite with a 0.05 wt% SWNT loading. The same chemistry and batch of HiPco SWNTs were used to compare the results with previously reported properties. The loading level of 0.05 wt% was evaluated since it was previously determined to afford materials with sufficient surface resistivity deemed necessary for ESC mitigation [10]. The data generated in this study as well as prior data based on SWNT loading effects [10] were subsequently examined using Beer's (absorbance vs. concentration) and Lambert's (absorbance vs. film thickness) laws taking into account reflectivity losses from the film surfaces. The α, another absorptive property, was also analyzed using these laws even though it encompasses a broad spectral region ranging from 250 to 2800 nm. Previous results had indicated that α also followed Beer's law [10]. The results of this analysis were used to generate simple predictive equations that are described herein. The ε is dependent on many factors such as surface finish, color, oxidation, aging, etc. Thus the effects of thickness and concentration upon ε are reported, but were not modeled.

2. Experimental

2.1. Single-walled carbon nanotubes (SWNTs)

SWNTs prepared by the HiPco process were obtained from Tubes@Rice and purified by heating at 250 °C for ~16 h in a high humidity chamber over moist air followed by Soxhlet extraction with hydrochloric acid (22.2 wt%) for ~24 h.

2.2. Alkoxysilane terminated amide acid synthesis (ASTAA)

The ASTAA of LaRC™ CP-2 was prepared as previously described by the reaction of 4,4′-hexafluoroisopropylidiene diphthalic anhydride with 1,3-bis-(3-aminophenoxy)benzene and end-capped with aminophenyltrimethoxysilane (~90% *meta*, ~10% *para*) at a 2.5% offset in *N*,*N*-dimethylacetamide (DMAc) [10]. The calculated number average molecular weight was ~27,700 g/mol.

2.3. SWNT–ASTAA mixture

Nanocomposite solutions were prepared as previously described by the addition of a mixture of SWNTs in DMAc that was sonicated at ambient temperature for ~2.5 h to a pre-weighed ASTAA/DMAc solution [10]. The mixture was stirred for ~16 h under nitrogen at room temperature prior to film casting.

2.4. Films

DMAc solutions of the ASTAAs (with and without

Table 1
Optical and thermo-optical properties at constant wt% SWNT loading

ID	SWNT (wt%)	Film thickness (μm)	%T@500 nm	A@500 nm[a]	α	ε
P1 [10]	0	38.0	86	0.0655	0.07	0.59
P2 [10]	0.03	38.0	67	0.1739	0.21	0.63
P3 [10]	0.05	41.0	59	0.2291	0.30	0.65
P4 [10]	0.08	38.0	53	0.2757	0.35	0.67
P5	0.05	17.5	75	0.1249	0.16	0.47
P6	0.05	22.5	71	0.1487	0.19	0.50
P7	0.05	35.0	65	0.1871	0.26	0.58
P8	0.05	37.5	62	0.2076	0.28	0.59
P9	0.05	55.0	54	0.2676	0.34	0.64
P10	0.05	67.5	47	0.3279	0.41	0.70
P11	0.05	82.5	39	0.4089	0.45	0.72
P12	0	25.0	87	0.0605	0.06	0.46
P13	0	30.0	87	0.0605	0.06	0.51
P14	0	32.5	87	0.0605	0.06	0.51
P15	0	40.0	86	0.0655	0.07	0.55
P16	0	60.0	84	0.0757	0.07	0.62
P17	0	72.5	81	0.0915	0.09	0.65
P18	0	87.5	79	0.1024	0.10	0.68

[a] $A = 2 - \log_{10} \%T$, air was used as the blank.

SWNTs as described above) were doctored onto clean, dry plate glass and dried to tack-free forms in a low humidity chamber at ambient temperature. The films on glass were stage cured in a forced air oven at 100, 200, and 300 °C for 1 h each. The films were subsequently removed from the glass plate and characterized.

2.5. Characterization

Inherent viscosities (η_{inh}) were obtained on a 0.5% (w/v) amide acid solution in DMAc at 25 °C. Film thickness was determined on a Testing Machines, Inc. digital micrometer. UV/VIS/near-IR spectra were obtained on thin films using a Perkin–Elmer Lambda 900 UV/VIS/near-IR spectrometer. ATR–FTIR spectra were obtained on thin films using a ThermoNicolet IR300 Spectrometer. Surface resistivity was determined according to ASTM D-257-99 using a Prostat® PSI-870 surface resistance and resistivity indicator operating at 9 V and reported as an average of three readings. The α was measured on thin films using an AZ Technology Model LPSR-300 spectroreflectometer with measurements taken between 250 and 2800 nm. Vapor-deposited aluminium on Kapton® film (1st surface mirror) was used as the reflective reference for air mass 0 per ASTM E903.

3. Results and discussion

3.1. Nanocomposite preparation

The objective of this work was to derive simple empirical relationships for the absorbance at 500 nm and α for this nanocomposite film system based on SWNT loading (concentration) and film thickness. This was of interest given that it is currently very difficult to prepare extremely thin films (<3 μ) that are required for Gossamer structures. Prior work relating SWNT loading and these properties revealed an adherence to Beer's law [10]. Beer's law was originally derived for solutions containing various concentrations of an absorbing species in a cell (typically matching quartz cuvettes) of a constant path length (typically 1 cm). It has been reported to be applicable to thin films as well; however, the plots resulted in a non-zero *y*-intercept that was presumably due to light scattering and reflection [14]. Similar results were observed for P1–P4 (Table 1) where losses associated with light scattering due to the film and SWNTs and reflectivity due to the film were not addressed [10]. It is known that scattering contributions to the absorption spectrum by SWNT bundles are very difficult to determine owing to the overall complexity of the SWNTs themselves (e.g. method of preparation and distribution of

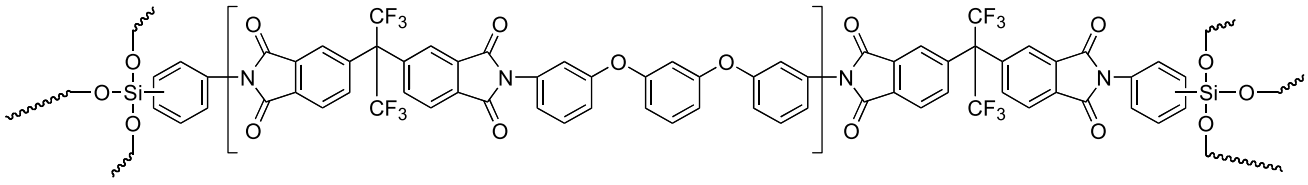

Fig. 1. Polyimide from alkoxysilane terminated amide acid of LaRC™ CP2.

different diameter, chirality, length, bundling, etc.) [13]. The thermo-optical (α and ε) and optical properties at 500 nm for P1–P4 are republished in Table 1 for the readers benefit and for use later in deriving the respective empirical relationships.

To determine thickness effects, additional nanocomposite films from alkoxysilane terminated amide acid (ASTAA) polymers of LaRC™ CP2 (Fig. 1) and purified HiPco SWNTs were prepared and characterized. This was done for both the pristine polymer and the nanocomposite with a SWNT loading level of 0.05 wt%.

In order to compare the results obtained here with prior results, the same batch of HiPco SWNTs were used. The elemental analysis of these SWNTs was 89% C, 0.5% H, and 1.8% Fe with the remaining mass balance being attributed to oxygen. The oxygen was presumably in the form of carbon–oxygen bonded species such as carboxylic acid and hydroxyl groups located at defect sites along the tube or at the tube ends [15,16]. The SWNTs were sonicated in solution for ~2.5 h and subsequently added to the premade ASTAA solution. This mixture was then stirred under low shear prior to casting unoriented films of varying thickness. The room temperature dried films were stage cured and imidized to 300 °C in flowing air prior to analysis.

It had been postulated that a chemical reaction would occur between the alkoxysilane endcap and functionalities on the SWNT [10]. However, direct observance of chemical bond formation has been difficult to ascertain due to the low amount of functional groups present. A model reaction was performed with 3-aminopropyldimethylethoxysilane to determine if a reaction with the SWNT would occur [10]. Analysis of this model compound by high resolution scanning electron microscopy (HRSEM) revealed a light organic coating on SWNTs. This coating was not present on the pristine SWNTs. The Raman spectra of the model compound and the pristine tubes were comparable except for some minor differences in the radial breathing mode. These differences have been observed by others and can be due to a number of factors [17–19]. Based on these results, a slight amount of direct bonding may have occurred to the SWNTs but is difficult to determine.

In the matrix the SWNTs were well dispersed with no visible large agglomerates as observed by HRSEM; however, localized regions of low and high SWNT concentration were evident [10]. Examination of these films by ATR–FTIR showed no difference in the spectra between the pristine film and the nanocomposites. By Raman spectroscopy, little difference was observed between the nanocomposites and the pristine tubes [10].

3.2. Optical and α properties

The effect of film thickness upon % transmission (%T) and absorbance (A, where $A = 2 - \log_{10}\%T$) at 500 nm and α for the pristine material and one containing a SWNT loading level of 0.05 wt% are reported in Table 1. Films P5–P11 were prepared from a single nanocomposite mixture of an ASTAA with an η_{inh} of 0.66 dl/g and a 0.05 wt% SWNT loading. As expected the α, ε, and absorbance at 500 nm increased with increasing film thickness. Initial plots of absorbance at 500 nm and α vs. film thickness were found to obey Lambert's law. Lambert's law is similar to Beer's law except that it examines the effect of thickness while holding concentration constant. As previously mentioned, loses due to reflectivity and light scattering were not taken into account with this initial plot.

For interest, the surface resistivity was 10^8 Ω/sq for P5–P8 and 10^7 Ω/sq for P9–P11. These values were comparable to P3 [10]. Film P5 had some surface areas where the readings were 10^{10} Ω/sq, implying that there were regions of low and high SWNT concentration.

Film thickness effects on %T at 500 nm and α for the neat polymer (P12–P18, Table 1) were also determined. The η_{inh} of the ASTAA was 0.94 dl/g with cured film thickness ranging from 25.0 to 87.5 μm. The %T at 500 nm and α did not vary appreciably for film thickness ranging from 25.0 to 40.0 μm (P12–P15) whereas ε increased ~20%. Like the SWNT containing films (P5–P11), adherence to Lambert's law was found when absorbance at 500 nm and α were initially plotted vs. film thickness. Reflectivity and light scattering losses were not addressed in these initial plots.

3.3. Calculated reflectivity loss

Both Beer's and Lambert's laws pertain to the absorbance at a particular wavelength of a species dissolved in a solution. These experiments are typically performed using matching quartz cuvettes with one cell containing a solvent blank so as to subtract out losses due to solvent and reflectance at the quartz–air interfaces. In this study, however, the solution is a solid polymer matrix. Consequently, the Fresnel reflection from the two polymer–air interfaces of the material had to be taken into account so this reflectance loss is not wrongly attributed to absorption or scattering by the medium (i.e. neat polymer) [20]. The fraction reflected from each surface can be calculated from

$$R = \left[\frac{(n_{\text{LaRC}^{\text{TM}}\ \text{CP-2}} - n_{\text{air}})}{(n_{\text{LaRC}^{\text{TM}}\ \text{CP-2}} + n_{\text{air}})}\right]^2$$

where R is the reflectivity and $n_{\text{LaRC}^{\text{TM}}\ \text{CP-2}} = 1.61$ and $n_{\text{air}} = 1$ are the indices of refraction of LaRC™ CP-2 [4] and air, respectively, resulting in $R = 0.0546$ per surface. Considering that the film has two air–polymer surfaces, the %T for a sample having zero absorbance was calculated as

$$\%T = 100(1 - 2R) = 89.1\%$$

Therefore, a modified definition of absorbance (A^*) was used where

$$A^* = 2 - \log_{10}\left(\frac{\%T}{0.891}\right) \quad (1)$$

Table 2
Modified absorbance at 500 nm and estimated SWNT concentration

ID	SWNT (wt%)	Estimated c_{SWNT} (mol/l)	Film thickness (μm)	A^*@500 nm[a]
P1	0	0	38.0	0.0152
P2	0.03	0.041	38.0	0.1237
P3	0.05	0.068	41.0	0.1789
P4	0.08	0.100	38.0	0.2255
P5	0.05	0.065	17.5	0.0747
P6	0.05	0.065	22.5	0.0985
P7	0.05	0.065	35.0	0.1368
P8	0.05	0.065	37.5	0.1573
P9	0.05	0.065	55.0	0.2173
P10	0.05	0.065	67.5	0.2776
P11	0.05	0.065	82.5	0.3587
P12	0	0	25.0	0.0102
P13	0	0	30.0	0.0102
P14	0	0	32.5	0.0102
P15	0	0	40.0	0.0152
P16	0	0	60.0	0.0255
P17	0	0	72.5	0.0412
P18	0	0	87.5	0.0521

[a] Eq. (1): $A^* = 2 - \log_{10}(\%T/0.891)$.

Here 0.891 refers to the 89.1% transmittance. Rearranging Eq. (1) afforded Eq. (2):

$$\%T = 89.1(10^{-A^*}) \quad (2)$$

The absorbance at 500 nm was then recalculated for P1–P18 using Eq. (1) in order to take into account losses due to this reflection with the values reported in Table 2.

To see if this modified absorbance calculation was valid, the absorbance at 500 nm was experimentally obtained using P12 and P14–P18 as the 'matching cuvette' for P6–P11 even though there were thickness differences. It was found that the experimentally obtained values differed by $\leq \pm 0.2\%$ from the calculated values obtained using Eq. (1). Based on the good agreement between experimental and calculated absorbance at 500 nm, Eq. (1) was used in this analysis with the results reported in Table 2. As a note, loss due to light scattering may have also occurred in these measurements.

3.4. Estimation of SWNT concentration

Since both the SWNT and the host polymer affect the transmission of light through the sample, analysis of the data must include the absorptivity of both. Thus, the absorptivity of the SWNT and host materials is defined as a_{SWNT} and a_{host}, respectively. Similarly, the concentrations of the SWNT and host materials are defined as c_{SWNT} and c_{host}, respectively. The expression for the modified absorbance (A^*) can then be written as:

$$A^* = (a_{host}c_{host} + a_{SWNT}c_{SWNT})b \quad (3)$$

where b is the film thickness. From this point there are many ways to treat the data ranging from simple to very complex. One way is to use wt% SWNT. However, to obtain absorptivity values in units that are traditionally found using the Beer–Lambert law equation, the wt% SWNT was mathematically converted into units of concentration (mol/l). This mathematical manipulation would then allow for comparison of absorptivity values determined from these films to those reported in the literature. The concentration for the polymer and the SWNTs were determined based on a 'simplification' of the components as described below.

First, the concentration of the host material (c_{host}) was calculated to be 2.10 mol/l by dividing the density (ρ) of the polymer (1.47 g/ml for LaRC™ CP-2) [3] by the repeat unit molecular weight (700.6 g/mol) and multiplying by 1000. Here it was assumed that the ρ of the modified LaRC™ CP-2 was comparable to that of LaRC™ CP-2, ignoring contributions from the endcapping group that was present at 5 mol%.

Secondly, the wt% SWNT loading was mathematically converted to concentration (mol/l) for c_{SWNT}. This was performed making several 'simple' assumptions. The first was that SWNTs could be thought of as 'essentially' an all carbon polymer as a first approximation to simplify data handling. It is recognized that this is a very simplistic view of SWNTs, but it allowed for a much easier data analysis. Based on this assumption, the SWNT repeat unit was taken as 12.0 g/mol negating SWNT chirality, various SWNT sizes, minor contributions afforded by oxygen, hydrogen, residual catalyst(s), etc. all of which may affect the SWNT optical properties. The second assumption was that the polymer matrix could be thought of as the 'solvent' that the SWNTs were 'dissolved' in. Using these assumptions, an example of determining the SWNT concentration is presented below.

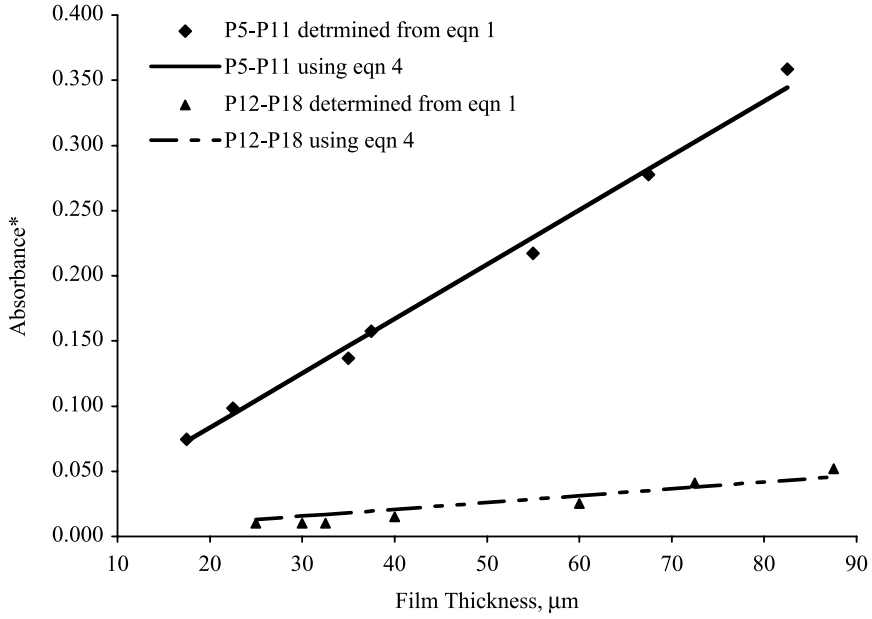

Fig. 2. Modified absorbance (A^*) at 500 nm vs. film thickness for neat (P12–P18) and SWNT-loaded films (P5–P11).

g SWNT $= 0.0018$ g approximate mol SWNT

$= 1.5 \times 10^{-4}$ mol

Repeat unit $MW_{ASTAA} = 736.6$ g/mol

Repeat unit $MW_{imide} = 700.6$ g/mol

$g_{ASTAA} = 3.392$ g

$g_{imide} = g_{ASTAA}(MW_{imide}/MW_{ASTAA}) = 3.227$ g

L_{imide} = (amount of Imide used/ρ of LaRC™ CP − 2)

$\times$(1 l/1000 ml)

$= 2.20 \times 10^{-3}$ l

$c_{SWNT} = 0.068$ mol/l for a 0.05 wt% SWNT loading

The c_{SWNT} was calculated for P2–P11 using the above method and reported in Table 2 along with the wt% SWNT loading.

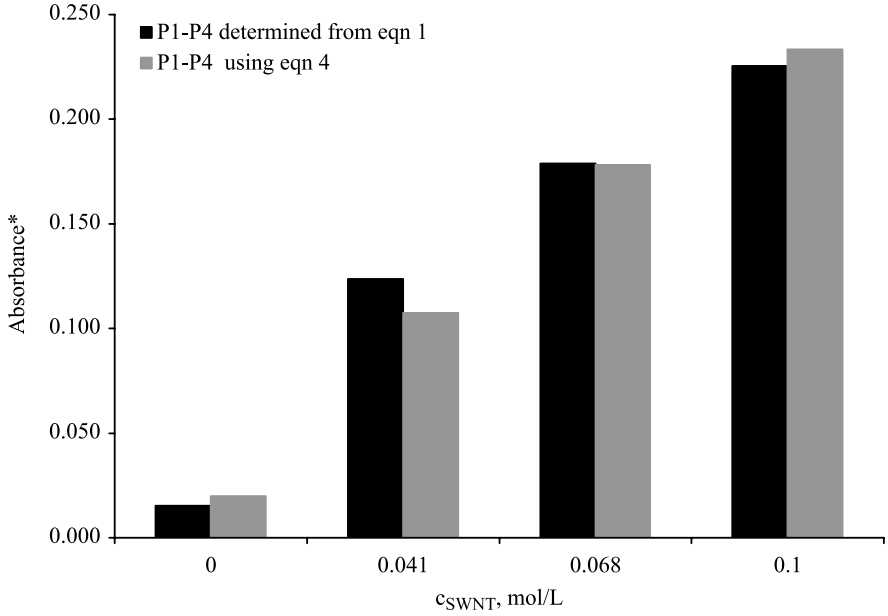

Fig. 3. Modified absorbance (A^*) at 500 nm vs. c_{SWNT} for approximately constant thickness films (P1–P4).

3.5. Analysis of absorbance (at 500 nm) measurements

The data in Table 2 can be summarized into three groups: (i) (P12–P18) variation of film thickness (b) for neat polymer ($c_{SWNT}=0$), (ii) (P1–P4) variation of c_{SWNT} for a constant film thickness (b, approximately equal to 38 μm), and (iii) (P5–P11) variation of film thickness (b) for a polymer with a constant concentration of SWNT ($c_{SWNT}=$ 0.065 mol/l). The first and third groups pertain to Lambert's law while the second group pertains to Beer's law. Since the modified absorbance at 500 nm (A^*), film thickness, and host and SWNT concentrations were known (Table 2); the only remaining unknowns in Eq. (3) were a_{host} and a_{SWNT}. Utilizing a nonlinear fitting approach in the Solver function in Microsoft Excel, initial estimates were made for these two values allowing a theoretical estimate of the modified absorbance at 500 nm for each sample. The difference between the empirical prediction of modified absorbance at 500 nm and the value of modified absorbance at 500 nm inferred from Eq. (1) was then calculated for each sample. These differences were then squared and summed. The values for a_{host} and a_{SWNT} were then adjusted to minimize the sum of these squares, thereby obtaining a best fit to all of the data simultaneously. Based on this analysis, empirical values for a_{host} and a_{SWNT} were determined to be 0.00025 and 0.056 l/(mol μm), respectively, for this particular class of nanocomposites at 500 nm. Thus Eq. (3) can be written as:

$$A^* = [0.00052\ \mu m^{-1} + (0.056\ l/(mol\ \mu m))c_{SWNT}]b \qquad (4)$$

Eq. (4) was then used to calculate the modified absorbance at 500 nm for the three groups with the results graphically compared to the data from Table 2 in Figs. 2 and 3.

Fig. 2 shows a comparison between Eq. (4) and the data for modified absorbance at 500 nm as a function of film thickness for both neat polymers and nanocomposites, P12–P18 and P5–P11, respectively. As expected, samples containing SWNTs have substantially higher absorbance at 500 nm than the neat samples. Furthermore, the absorbance at 500 nm increased with increasing film thickness for samples containing SWNTs as expected. However, it was surprising that the neat samples exhibited an increased absorbance at 500 nm with increasing film thickness. This implied that the host material (polymer) was absorbing (or possibly scattering) the incident light. Fig. 3 shows a comparison between Eq. (4) and the data for modified absorbance at 500 nm vs. increasing c_{SWNT}. This graph is shown as a bar graph instead of a line graph because all of the samples were not exactly the same thickness. The expected trend of increasing absorbance with increasing c_{SWNT} was observed.

Generally, the agreement between Eq. (4) and the data from Table 2 in Figs. 2 and 3 was good. The resulting fit values were $a_{host}=0.00025\pm0.00002$ l/(mol μm) and $a_{SWNT}=0.056\pm0.002$ l/(mol μm). The average deviation between the data and Eq. (4) (fit standard error) for absorbance at 500 nm was 0.008. Based on this fit standard error, the 95% confidence level of statistical uncertainty in Eq. (4) was estimated to be ±0.005 for the modified absorbance at 500 nm, and ±1 for $\%T$ at 500 nm using Eq. (2).

It has been reported that the a_{SWNT} at 500 nm for a different batch of as-produced HiPco SWNTs 'dissolved' or 'suspended' in 1,2-dichlorobenzene was 0.0286 l/(mg cm) [12]. Mathematical conversion of 0.056 l/(mol μm) for a_{SWNT} at 500 nm obtained for the HiPco SWNTs used in this study to the same units [l/(mg cm)] afforded a value of 0.046. This is ~60% greater than the reported value, but is of the same order of magnitude and was reasonable given that the SWNTs were from a different HiPco batch, purified, and suspended in a solid polymer matrix in addition to the relatively 'simplified' manner of treating the data. It has been reported that functionalized SWNTs (produced by arc discharge) were insensitive to the medium (solution vs. film) [13] thus allowing for comparisons to be made. An average a_{SWNT} at 500 nm in solution for these amide functionalized SWNTs (produced by the arc-discharge method) has been reported as 0.0074 l/(mg cm) [13]. A higher estimated a_{SWNT} at 500 nm of 0.097 l/(mg cm) was reported for defunctionalized arc discharge prepared SWNTs [21]. The higher value was suggested to be due to scattering effects due to larger bundles. As has been suggested by the various reports and observed in this study, values for a_{SWNT} at 500 nm are affected by the type of SWNT preparative and purification methods, distribution of sizes (bundles, diameter, and length), chirality, dispersal in the medium, light scattering contributions, etc. [13]. In addition, it is recognized that the optical properties of the SWNTs are complex and dependent upon many factors.

For certain types of Gossamer spacecraft, an infinitely thin film (thickness approaching 0) may be desired. Using Eq. (4), the modified absorbance at 500 nm would approach zero as the thickness approached 0 and is independent of c_{SWNT}. Using this result in Eq. (2), the $\%T$ at 500 nm would be approximately 89%, which is comparable to that of the pristine material of similar thickness. Of course, these two equations are representative only of this particular batch of polymer-SWNT nanocomposites. However, the overall methodology of this simplified approach does provide a first-order predictive approximation that may be useful when applied to other polymer-SWNT systems.

3.6. Solar absorptivity

As was found with the absorbance at 500 nm, α was found to obey both Beer's and Lambert's laws. The α encompasses the spectral region ranging from 250 to 2800 nm. A semi-empirical equation for α was chosen and best fit to the data using a nonlinear fitting approach in the Solver function in Microsoft Excel resulting in Eq. (5):

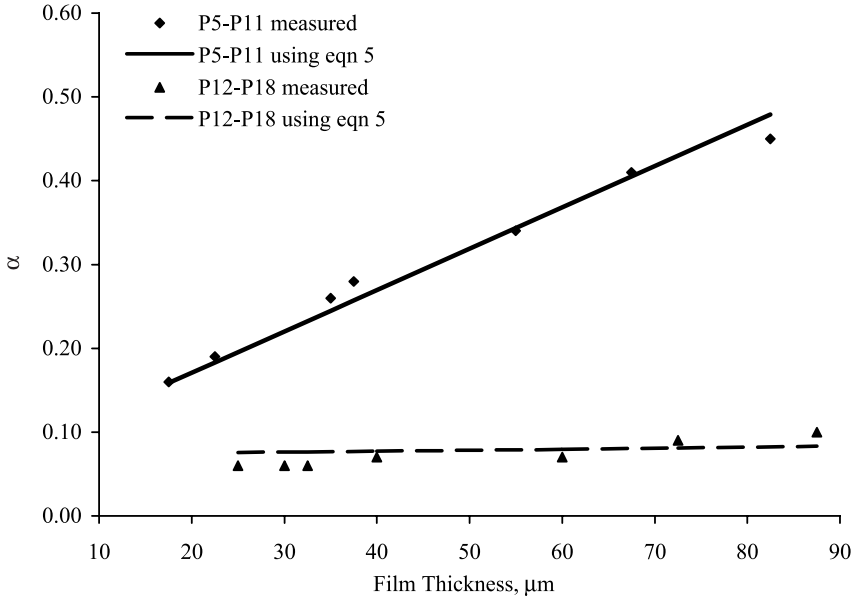

Fig. 4. α vs. film thickness for neat (P12–P18) and SWNT-loaded films (P5–P11).

$$\alpha = 0.07 + b[(0.000058\ \text{l/(mol}\ \mu\text{m)})c_{\text{host}} + (0.074\ \text{l/(mol}\ \mu\text{m)})c_{\text{SWNT}}] \quad (5)$$

where $c_{\text{host}} = 2.10$ mol/l, b is in microns, and c_{SWNT} is in mol/l. The above equation predicts α with an uncertainty of ± 0.01 with 95% confidence. Fig. 4 shows good agreement between the data in Table 1 and Eq. (5) for films where the thickness was varied. The α vs. c_{SWNT} relationship (P1–P4) was shown as a bar graph due to one sample not being of the same thickness as previously discussed. Similar agreement was found by comparing Eq. (5) and data in Table 1 vs. c_{SWNT} (Fig. 5).

Based on Eq. (5), an infinitely thin film (thickness approaching 0) based on this material system would exhibit an α of 0.07 and is independent of c_{SWNT} as was seen for the modified absorbance at 500 nm (Eq. (4)). This result is comparable to that of the pristine material of similar thickness. As previously stated for the treatment of the absorbance at 500 nm data, Eq. (5) is unique to this particular batch of nanocomposites. However, the methodology does allow for the development of an empirical relationship to predict α on a first order approximation that may be useful for other polymer SWNT nanocomposites of comparable loadings.

4. Summary

Optical and thermo-optical properties were measured for

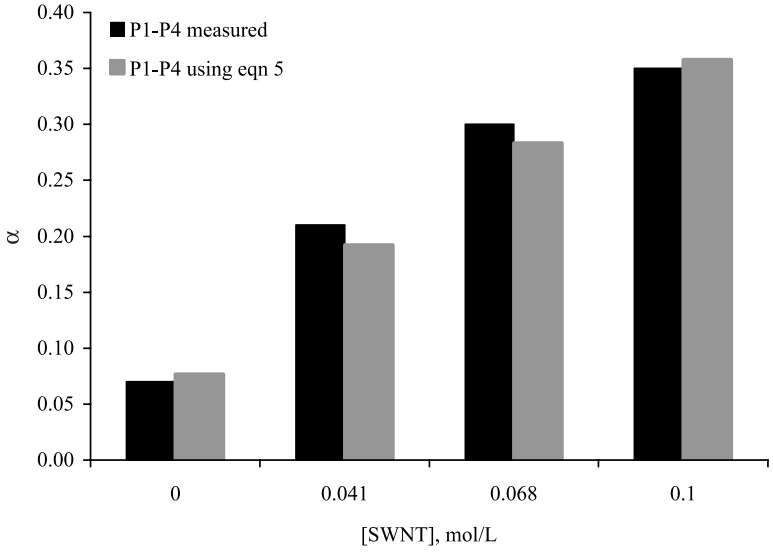

Fig. 5. α vs. c_{SWNT} for approximately constant thickness films (P1–P4).

nanocomposite films prepared from alkoxysilane terminated amide acid polymers of LaRC™ CP-2 and HiPco SWNTs. Both film thickness and c_{SWNT} were varied. The absorbance at 500 nm and α exhibited a linear dependence upon c_{SWNT} at constant film thickness and with varying film thickness at constant c_{SWNT}, respectively. These properties were found to obey Beer's and Lambert's laws, respectively. Empirical equations were developed for absorbance at 500 nm and α using a nonlinear fitting approach in the Solver function in Microsoft Excel. Predicted values for both were in good agreement with the data. The molar absorptivity at 500 nm determined for the HiPco SWNTs used in this study based on this approach was of the same order of magnitude as that determined for a different batch of HiPco SWNTs in solution.

The use of trade names of manufacturers does not constitute an official endorsement of such products or manufacturers, either expressed or implied, by the National Aeronautics and Space Administration.

References

[1] Jenkins CHM. Gossamer spacecraft: membrane and inflatable structures technology for space applications. vol. 191. American Institute of Aeronautics and Astronautics; 2001.

[2] Watson KA, Palmieri FL, Connell JW. Macromolecules 2002;35:4968.

[3] SRS Technologies, Huntsville, AL 35806, http://www.stg.srs.com/atd/polyimidesales/cp_prop.htm.

[4] Paasi J. Research Note, http://www.vtt.fi/tuo/45/tuloksia/surface_resistance.pdf, 19; 2002.

[5] Park C, Ounaies Z, Watson KA, Crooks RE, Smith Jr JG, Lowther SE, et al. Chem Phys Lett 2002;364:303.

[6] Watson KA, Smith Jr JG, Connell JW. Soc Adv Mater Process Eng Tech Conf Ser 2001;33:1551.

[7] Smith Jr JG, Watson KA, Thompson CM, Connell JW. Soc Adv Mater Process Eng Tech Conf Ser 2002;34:365.

[8] Glatkowski P, Mack P, Conroy JL, Piche JW, Winsor P. US Patent 6,265,466 B1, Eikos, Inc, 24; 2001.

[9] Ounaies Z, Park C, Wise KE, Siochi EJ, Harrison JS. Comp Sci Technol 2003;63:1637.

[10] Smith Jr JG, Connell JW, Delozier DM, Lillehei PT, Watson KA, Lin Y, et al. Polymer 2004;45:825.

[11] Watson KA, Ghose S, Delozier DM, Smith Jr JG, Connell JW. Polymer 2005;46.

[12] Bahr JL, Mickelson ET, Bronikowski MJ, Smalley RE, Tour JM. Chem Commun 2001;193.

[13] Bing Z, Lin Y, Huaping L, Huang W, Connell JW, Allard LF, et al. Phys Chem B 2003;107:13588.

[14] Hull CC, Crofts NC. Ophthal Physiol Opt 1996;16:150.

[15] Hu H, Bhowmik P, Zhao B, Hamon MA, Itkis ME, Haddon RC. Chem Phys Lett 2001;345:25.

[16] Mawhinney DB, Naumenko V, Kuznetsova A, Yates JT, Liu J, Smalley RE. Chem Phys Lett 2000;324:213.

[17] Bahr JL, Tour JM. Chem Mater 2001;13:3823.

[18] Bahr JL, Yang J, Kosynkin DV, Bronikowski MJ, Smalley RE, Tour JM. J Am Chem Soc 2001;123:6536.

[19] Holzinger M, Abraham J, Whelan P, Graupner R, Ley L, Hennrich F, et al. Am Chem Soc 2003;125:8566.

[20] (a) Meyer-Arendt JR. Introduction to classical and modern optics. Englewood Cliffs, NJ Prentice-Hall; 1972, p. 305–311.
(b) Hecht E. Optics. 4th ed. Reading, MA Addison-Wesley; 2001.

[21] Fu K, Huang W, Lin Y, Riddle LA, Carroll DL, Sun Y-P. Nano Lett 2001;1:439.